2-1-2017

Mosaic expression of Atrx in the mouse central nervous system causes memory deficits

Renee J. Tamming
Western University

Jennifer R. Siu
Western University

Yan Jiang
Western University

Marco A. M. Prado
Western University

Frank Beier
Western University

See next page for additional authors

Mosaic expression of *Atrx* in the central nervous system causes memory deficits

Renee J. Tamming[1,2], Jennifer R. Siu[1,3], Yan Jiang[1,2], Marco A.M. Prado[3,4], Frank Beier[1,3], and Nathalie G. Bérubé[1,2,5]

[1]Children's Health Research Institute, London, Ontario, Canada. [2]Departments of Paediatrics, Biochemistry, and Oncology, Schulich School of Medicine and Dentistry, the University of Western Ontario, Victoria Research Laboratories, London, Ontario, Canada. [3]Department of Physiology and Pharmacology, Schulich School of Medicine and Dentistry, the University of Western Ontario, London, Ontario, Canada. [4]Department of Anatomy & Cell Biology and Robarts Research Institute, the University of Western Ontario, London, Ontario, Canada.

[5]**Corresponding author:** nberube@uwo.ca

Key words: ATRX, central nervous system, mouse models, neurobehaviour

Summary statement: Heterozygous expression of the X-linked gene *Atrx* in the mouse brain causes deficits in spatial, contextual fear and object recognition memory.

Disease Models & Mechanisms • DMM • Advance article

Abstract

The rapid modulation of chromatin organization is thought to play a critical role in cognitive processes such as memory consolidation. This is supported in part by the dysregulation of many chromatin remodeling proteins in neurodevelopmental and psychiatric disorders. A key example is *ATRX*, an X-linked gene commonly mutated in individuals with syndromic and non-syndromic intellectual disability (ID). The consequences of *Atrx* inactivation on learning and memory have been difficult to evaluate due to the early lethality of hemizygous-null animals. In this study we evaluated the outcome of brain-specific *Atrx* deletion in heterozygous female mice. The latter exhibit a mosaic pattern of ATRX protein expression in the CNS due to the location of the gene on the X chromosome. While the hemizygous male mice die soon after birth, heterozygous females survive to adulthood. Body growth is stunted in these animals and they have low circulating levels of insulin growth factor 1 (IGF-1). In addition, they are impaired in spatial, contextual fear, and novel object recognition memory. Our findings demonstrate that mosaic loss of ATRX expression in the CNS leads to endocrine defects, decreased body size and has a negative impact on learning and memory.

Disease Models & Mechanisms • DMM • Advance article

Introduction

Alpha thalassemia mental retardation, X-linked, or ATR-X syndrome, is an intellectual disability (ID) disorder that arises from mutations in the *ATRX* gene (OMIM 301040). This rare syndrome is characterized by severe developmental delay, hypotonia, mild α-thalassemia, and moderate to severe ID (Gibbons et al., 1995). A recent study screened a cohort of nearly 1000 individuals with ID using targeted next-generation sequencing and identified *ATRX* variants as one of the most common cause of ID, reinforcing its importance in cognition (Grozeva et al., 2015). The ATRX protein is a SWI/SNF-type chromatin remodeler. The N-terminal region of the protein contains a histone reader domain that mediates interaction of the protein with histone H3 trimethylated at lysine 9 (H3K9me3) and unmethylated at lysine 4 (H3K4me0) (Dhayalan et al., 2011). A SWI/SNF2-type helicase domain is located in the C-terminal half of the protein and confers ATP-dependent chromatin remodeling activity (Aapola et al., 2000; Gibbons et al., 1997; Picketts et al., 1996). Several proteins have been shown to interact with ATRX, including MeCP2, HP1α, EZH2 and DAXX (Berube et al., 2000; Cardoso et al., 1998; Nan et al., 2007; Xue et al., 2003). DAXX is a histone chaperone for histone variant H3.3. In association with ATRX, DAXX deposits H3.3-containing nucleosomes at telomeres and pericentromeric heterochromatin (Drane et al., 2010; Lewis et al., 2010).

Several studies have previously implicated ATRX in the regulation of gene expression through a variety of mechanisms. Chromatin immunoprecipitation (ChIP) sequencing for ATRX in human erythroblasts showed that the protein tends to bind GC-rich regions with high tendency to form G-quadruplexes. For example, ATRX was found to bind tandem repeats within the human α-globin gene cluster and it was suggested that reduced expression of α-globin might be caused by replication-dependent mechanisms that would affect the expression of nearby genes (Law et al., 2010). The induction of replication stress was in fact detected *in vivo* upon inactivation of *Atrx* in either muscle or brain (Leung et al., 2013; Watson et al., 2013). More recently our group demonstrated that loss of ATRX corresponds to decreased H3.3 incorporation and increased PolII occupancy in GC-rich gene bodies, including *Neuroligin 4*, an autism susceptibility gene (Levy et al., 2015).

While the mechanisms by which ATRX modulates chromatin and genes is starting to be resolved, its function in neurons and cognitive processes is still obscure. To address this question, we generated mice with conditional inactivation of *Atrx* in the central nervous system (CNS) starting at early stages of neurogenesis. While hemizygous male progeny died shortly after birth, heterozygous female mice (here on called *Atrx*-cHet) that exhibit mosaic expression of ATRX caused by random X-inactivation, survived to adulthood, allowing the investigation of neurobehavioural outcomes upon inactivation of *Atrx* in the brain.

Results

Survival to adulthood depends on the extent of *Atrx* deletion in the CNS.

Conditional inactivation of *Atrx* is required to elucidate its functions in specific tissues, since general inactivation of the gene is embryonic lethal (Garrick et al., 2006). We thus generated mice with Cre recombinase-mediated deletion of *Atrx* floxed alleles in the CNS using the Nestin-Cre driver line of mice. Hemizygous male mice (*Atrx*-cKO) died by postnatal day (P)1 (**Figure 1A**). Due to random X-inactivation in females, *Atrx* is only expressed from one of the alleles in any specific cell, resulting in a mosaic pattern of expression in the brain of *Atrx*-cHet mice (e.g. if the floxed allele is the active allele, these cells are functionally null for *Atrx*; however, if the floxed allele is the silent one, cells are functionally wild type for *Atrx*). This was validated by RT-qPCR with *Atrx* primers in exon 17 and the excised exon 18, showing approximately 50% decreased *Atrx* expression in the cortex and hippocampus of Atrx-cHet mice compared to littermate controls (**Figure 1B**). Moreover, a mosaic pattern of ATRX protein expression was observed by immunofluorescence staining of the hippocampus and medial prefrontal cortex (**Figure 1C,D)**. This was quantified in the medial prefrontal cortex in three pairs of control and cKO animals (**Figure 1E)**. Hematoxylin and eosin staining of control and *Atrx*-cHet brain sections did not reveal major histological alterations in the CA1, CA3 and mPFC regions (**Figure 1F**). These results demonstrate that inactivation of *Atrx* throughout the CNS is perinatal lethal but that *Atrx* deletion in approximately half of cells allows survival of the female heterozygous mice to adulthood.

Mosaic inactivation of *Atrx* in the CNS impedes normal body growth.

The weight of Atrx-cHet mice was measured weekly over the course of the first 24 postnatal weeks. The data show that the Atrx-cHet mice weigh significantly less than control mice over this time period ($F= 17.87$, $p=0.0003$) (**Figure 2A,B**). Alcian blue and alizarin red skeletal staining of P17 mice reveal that the Atrx-cHet skeletons are smaller than those of the control (**Figure 2C**). Tibia, femur and humerus bones were also measured and found to be significantly shorter in the Atrx-cHet mice compared to littermate controls (**Figure 2D**).

We previously reported that deletion of *Atrx* in the developing mouse forebrain and anterior pituitary leads to low circulating levels of IGF-1 and thyroxine (T4) (Watson et al., 2013). Some evidence suggests that T4 regulates the prepubertal levels of IGF-1, while after puberty this regulation is largely mediated by growth hormone (GH) (Xing et al., 2012). Given that the Atrx-cHet mice are smaller than control mice, we examined the levels of T4, IGF-1 and GH in the blood by ELISA assays. We observed no significant difference in T4 and GH levels between P17 Atrx-cHet mice and control littermates. However, there was a large (80%) and significant decrease in IGF-1 levels (**Figure 2E**). Thus, reduced body size of the Atrx-cHet mice correlates with low circulating IGF-1 levels.

Hindlimb clasping phenotype in Atrx-cHet mice.

The *Atrx*-cHet mice displayed increased hindlimb clasping compared to controls, with more than 90% exhibiting limb clasping by three months of age ($F=20.78$, $p<0.0001$) (**Figure 3A**). In the open field test, the distance traveled was not significantly different between control and *Atrx*-cHet mice indicating that activity and locomotion are normal ($F=0.20$, $p=0.66$) (**Figure 3B**). Anxiety levels were also normal, based on time spent in the centre of the open field apparatus (($F=0.84$, $p=0.44$) (**Figure 3C**). Similarly, their performance in the elevated plus maze paradigm revealed no significant difference in the amount of time control and *Atrx*-cHet mice spent in the open vs. closed arms ($F=0.68$, $p=0.41$) (**Figure 3C,D**). We conclude that the Atrx-cHet mice are not hyper- or hypo-active and do not exhibit excessive anxiety, but the increased level of hindlimb clasping behaviour is suggestive of neurological defects.

Atrx-cHet mice have normal working memory but deficits in object recognition memory.

Given that *ATRX* mutations are linked to ID, we next evaluated memory in *Atrx*-cHet mice using various established paradigms. We first tested short-term working memory in the Y-maze task (de Castro et al., 2009). No difference was detected between control and *Atrx*-cHet mice in percent alternation, nor in the number of entries into the arms, suggesting that working memory is normal in *Atrx*-cHet mice (t=0.05, p=0.96) (**Figure 4A**). We then tested the Atrx-cHet mice in the spontaneous novel object recognition task that mainly involves the prefrontal cortex and hippocampus (Ennaceur and Delacour, 1988). In rodents, the natural tendency to seek out and explore novelty leads to a preference for the novel over the familiar object, indicating recognition memory of the familiar object (Bevins and Besheer, 2006). During the habituation period, both control and *Atrx*-cHet mice spent approximately 50% of the allotted time with each individual object (**Figure 4B**). In the course of the short-term memory test (1.5 hours), control mice spent approximately 70% of their time with the novel object while *Atrx*-cHet mice still spent ~50% of their time with each object, suggesting an inability to remember the familiar object (**Figure 4B**). Similar results were obtained in the long-term memory test (24 hours). The total amount of time spent interacting with the objects was unchanged between control and *Atrx*-cHet mice during all three tests, ruling out visual or tactile impairment.

Atrx-cHet mice display deficits in contextual fear and spatial memory.

To evaluate contextual fear memory, mice were placed in a box with distinctive black and white patterns on the sides for 3 minutes and shocked after 2.5 minutes. Twenty-four hours later they were placed back into the same box with the same contextual cues and the time spent freezing was measured at 30s intervals. The data show that the *Atrx*-cHet mice spent less time freezing than control mice (F=28.57, p<0.0001), and the total percentage of immobility time was significantly lower for *Atrx*-cHet mice, indicating impaired fear memory in these mice (t=5.35, p<0.0001) (**Figure 4C**).

The Morris water maze paradigm was next utilized to evaluate hippocampal-dependent spatial memory (Morris, 1984). During the four days of training, the *Atrx*-cHet mice took significantly more time finding the target platform while swimming a

longer distance compared to control mice (latency $F=31.44$, $p<0.0001$; distance $F=12.29$, $p<0.01$) (**Figure 5A**). The *Atrx*-cHet mice also swam more slowly than control mice ($F=15.40$, $p<0.001$) (**Figure 5A**). During testing on the fifth day, the platform was removed and the time spent in each quadrant was recorded as a measure of spatial memory. Whereas control mice spent significantly more time in the target quadrant than the left or opposite quadrant ($F=4.70$, $p<0.01$), *Atrx*-cHet mice showed no preference for the target quadrant ($F=0.75$, $p=0.53$) (**Figure 5B**). The results suggest that spatial learning and memory might be impaired in the *Atrx*-cHet mice. The non-cued Morris water maze was used to determine whether motivational or sensorimotor defects contribute to the phenotype seen in the non-cued version of the test. The data demonstrate that while the control mice quickly learn to correlate the cue with the platform, the *Atrx*-cHet mice were unable to do so ($F=14.09$, $p<0.01$) (**Figure 5C**). We noticed that the mice failed to show normal signs of aversion to water during this task, preferring to be swimming rather than to climb on the platform during training, even jumping back into the water after being placed on the platform.

Atrx-cHet mice have normal motor endurance and motor memory.

Given that the *Atrx*-cHet mice swam slower than controls in the Morris water maze task, we considered that perhaps the test was confounded by motor skills deficits. To clarify this issue, we further examined endurance and motor skills in the mutant mice. We found that motor function and balance measured in the Rotarod task were not significantly different in *Atrx*-cHet mice during any of the trials ($F=3.02$, $p=0.09$) (**Figure 6A**). *Atrx*-cHet mice also performed similarly to controls in the treadmill task ($t=0.34$, $p=0.73$) (**Figure 6B**). In contrast, *Atrx*-cHet mice exhibited decreased forelimb grip strength, normalized to body weight ($t=2.80$, $p<0.05$) (**Figure 6C**).

Discussion

This study demonstrates that deletion of *Atrx* in the CNS leads to endocrine defects and behavioural abnormalities. Specifically, we see impairments in spatial learning and memory in the Morris water maze, in contextual fear conditioning, and in novel object recognition.

We previously reported that mice lacking ATRX expression in the embryonic mouse forebrain have an average lifespan of 22 days (Watson et al., 2013). It is thus not surprising that inactivation of *Atrx* using the *Nestin-Cre* driver (which mediates deletion in the majority of CNS cells) is neonatal lethal. In contrast, the Atrx-cHet female mice survived to adulthood, likely because roughly half of all *Nestin*-expressing cells, as well as their progeny are spared. Mosaic loss of ATRX in Atrx-cHet female mice still negatively affects development, as the mice are smaller compared to littermate controls and the length of long bones is decreased. As the *NestinCre drive does* not promote Cre expression in bone progenitors (Wiese et al., 2004), this phenotype might result from the low level of circulating IGF-1 in these mice. The reason for low IGF-1 is difficult to pinpoint in our mice, It has been shown that mice expressing Cre under the control of the *Nestin* promoter are smaller due to a decrease in mouse GH (Declercq et al., 2015). However, in our hands, GH levels are normal in the Atrx-cHet mice. Given the normal levels of both T4 and GH, there could be unanticipated expression of Cre in the liver that affects IGF-1 production. Examining the potential off-target expression of Cre will be required to elucidate the mechanism of IGF-1 downregulation in these mice.

The *Atrx*-cHet mice displayed a variety of behavioural abnormalities. We initially noticed that the mice display excessive hindlimb clasping, which could indicate neurological impairment (Guy et al., 2001). This prompted us to perform additional tests to assess neurobehaviour of the mice. We observed no change in general activity or anxiety using the open field test and elevated plus maze, respectively, and no change in working memory in the Y-maze task. The *Atrx*-cHet mice exhibited increased latency to reach the platform in the Morris water maze task, which might indicate a defect in spatial memory. However, the findings are difficult to interpret since Atrx-cHet mice swam at a lower speed, which could indicate a problem with their ability to swim rather than with memory. It was previously reported that mice lacking MeCP2

protein, an established interactor of ATRX in the brain exhibit navigational difficulties in the Morris water maze (Stearns et al., 2007). Significant differences in swimming ability made it difficult to conclude whether the increased latency to the platform was due to motor or cognitive deficits, similar to our findings with the *Atrx*-cHet mice. While we did not observe defective motor skills in the Rotarod or treadmill tests or decreased activity in the open field test (above), we noticed that the mice failed to show normal signs of aversion to water during this task, preferring to be swimming rather than to climb on the platform during training, even jumping back into the water after being placed on the platform. We attempted to test the mice in the Barnes maze, another spatial learning and memory test, however the heterozygote mice tended to jump off the edge of the maze. Based on these observations, it will be important in the future to perform additional tests that gauge the level of motivation in these mice.

Despite these issues, which might require further experimentation for a full understanding, we obtained supporting evidence that memory is affected in the Atrx-cHet mice in the contextual fear the novel object recognition tasks. Additional support comes from a previous study done in a mouse model of Chudley-Lowry syndrome associated with reduced expression of ATRX (Nogami et al., 2011). The authors of that study reported an impairment in contextual fear memory and suggested that ATRX may play a role in regulation of adult born neurons. Our results show defects not only in contextual fear memory, but also in novel object recognition and potentially the Morris water maze task. This may indicate a role for ATRX not only in adult-born neurons, but perhaps also in the amygdala, hippocampus and the rest of the medial temporal lobe, structures which are vital for the tasks impaired in the *Atrx*-cHet mice (Logue et al., 1997; Phillips and LeDoux, 1992; Wan et al., 1999).

The DAXX protein is a well-established interactor of ATRX. While the behaviour of DAXX knockout mice has not yet been investigated, a study previously demonstrated that DAXX binds with ATRX to the promoters of several immediate early genes upon activation of cortical neuronal cultures (Michod et al., 2012). DAXX was also shown to be critical for the incorporation of histone H3.3 at these gene promoters, supporting a potential role for DAXX and ATRX the initial steps of memory consolidation. EZH2, a member of the PRC2 complex that mediates H3K27 trimethylation is another putative binding partner of ATRX (Cardoso et al., 1998; Margueron et al., 2009). Inducible deletion of the *Ezh2* gene in neural progenitor cells

in the adult brain caused impaired spatial learning and memory and contextual fear memory, suggesting that EZH2 (potentially with ATRX) provides important cues in adult neural progenitor cells (Zhang et al., 2014).

We emphasize that these mice do not model the ATR-X syndrome, where only males are affected and females exhibit 100% skewing of X chromosome inactivation and are therefore largely unaffected. Rather, the Atrx-cHet mice are a useful tool to probe ATRX function in the CNS. Overall, our study presents compelling evidence that ATRX is required in the mouse CNS for normal cognitive processes and sets the stage for additional investigations delving into the mechanisms by which it regulates chromatin structure and gene expression in neurons in the context of learning and memory.

Methods

Animal care and husbandry. Mice were exposed to a 12-hour-light/12-hour-dark cycle and with water and chow *ad libitum*. The *Atrx*^{loxP} mice have been described previously (Berube et al., 2005). *Atrx*^{loxP} mice (129svj) were mated with mice expressing Cre recombinase under the control of the *Nestin* gene promoter (Bl6) (Tronche et al., 1999). The progeny include hemizygous male mice that produce no full-length ATRX protein in the CNS (*Atrx*$^{f/y}$ *Cre*$^{+}$) and heterozygous female mice with approximately half of cells lacking ATRX protein due to the random pattern of X inactivation (*Atrx*$^{f/+}$ *Cre*$^{+}$). Male and female littermate floxed mice lacking the Cre allele were used as controls. Genotyping of tail biopsies for the presence of the floxed and Cre alleles was performed as described previously (Berube et al., 2005; Seah et al., 2008). All procedures involving animals were conducted in accordance with the regulations of the Animals for Research Act of the province of Ontario and approved by the University of Western Ontario Animal Care and Use Committee (2008-041). Behavioural assessments started with less demanding tasks (grip force, open field tests) to more demanding ones (Morris water maze). Experimenters followed ARRIVE guidelines: mouse groups were randomized, they were blind to the genotypes, and software-based analysis was used to score mouse performance in most of the tasks. All experiments were performed between 9:00 AM and 4:00 PM.

Immunofluorescence staining. Mice were perfused and the brain fixed for 72 hours with 4% paraformaldehyde in PBS and cryopreserved in 30% sucrose/PBS. Brains

were flash frozen in Cryomatrix (Thermo Scientific) and sectioned as described previously (Ritchie et al., 2014). For immunostaining, antigen retrieval was performed by incubating slides in 10 mM sodium citrate at 95°C for 10 min. Cooled slides were washed and incubated overnight in anti-ATRX rabbit polyclonal antibody (1:200, H-300 Santa Cruz Biotechnology Inc. #SC-15408) (Watson et al., 2013) diluted in 0.3% Triton-X/PBS. Sections were washed and incubated with goat anti-rabbit-Alexa Fluor 594 (Life Technologies) for one hour. Sections were counterstained with DAPI and mounted with SlowFade Gold (Invitrogen). Cell counts were done in 3 control/KO littermate-matched pairs was done in a blinded manner.

Microscopy. All images were captured using an inverted microscope (DMI 6000b, Leica) with a digital camera (ORCA-ER, Hamamatsu). Openlab image software was used for manual image capture, and images were processed using the Volocity software (PerkinElmer).

Hematoxylin and eosin staining. Brain cryosections (8 µm) from three month old mice were rehydrated in 70% ethanol for 2 min then tap water for 5 min. They were then placed in CAT hematoxylin (Biocare) for 2 min, placed under running tap water for 1 min, and set in filtered Tasha's Bluing Solution (Biocare) for 30 s. The slides were placed under running tap water for 10 min and set in filtered Eosin Y (Fisher Scientific) for 2 min. Immediately after the cells were dehydrated by two baths in 70% ethanol for 30 s each, then one in 90% ethanol for 1 min and two baths in 100% ethanol for 2 min each. The slides were placed in Xylene 3x for 5 min and mounted with Permount immediately after.

qRT-PCR. Total RNA was isolated from control and Atrx cHet or control rostral cortex and hippocampus using the RNeasy Mini Kit (QIAGEN) and reverse transcribed to cDNA using 1 µg RNA and SuperScript II Reverse Transcriptase (Invitrogen). cDNA was amplified in duplicate using primers under the following conditions: 95°C for 10 s, 55°C for 20 s, 72°C for 30 s for 35 cycles. Primers detected *Atrx* exons 17 and 18. Standard curves were generated for each primer pair. Primer efficiency was calculated as $E = (10^{-1/slope} - 1) * 100\%$, where a desirable slope is -3.32 and $R^2 > 0.990$. All data were corrected against β-actin.

ELISA assays. Blood was collected from the inferior vena cava of P17 mice. 100 µL of 0.5 M EDTA pH 7.0 per mL of blood collected were added to the blood sample and

centrifuged at 15,000 rpm for 10 min at 4°C. Plasma supernatant was collected and kept frozen at -80°C. Plasma IGF-1 level was measured using a mouse IGF-1 ELISA kit (R&D Systems, #MG100). Plasma growth hormone (GH) (Millipore, #EZRMGH-45K) and thyroxine (T4) (Calbiotech, #T4044T) were also measured by ELISA according to the manufacturer's instructions.

Bone staining and measurements. Skinned and eviscerated P17 mouse carcasses were fixed overnight in 95% ethanol and transferred to acetone overnight (Ulici et al., 2009). Fixed skeletons were stained in a 0.05% Alizarin Red, 0.015% Alcian Blue, 5% acetic acid in 70% ethanol solution for 7 to 14 days. Stained skeletons were cleaned in decreasing concentrations of potassium hydroxide (2%, 1% and 0.5%) for several days and stored in 50:50 70% ethanol/glycerol solution. Alcian blue and alizarin red stained skeletons were imaged using an Olympus SP-57OUZ digital camera. The tibia, femur and humerus lengths as well as skull widths and foot lengths from at least four different littermate pairs from both mouse models were imaged using the Zeiss Stereo Zoom Microscope Stemi SV6 and measured with a ruler accurate to 0.1 mm.

Hindlimb clasping, grip force, rotarod, treadmill, and open field tests. Hindlimb clasping was measured by lifting mice up by the base of the tail. Clasping was scored on a scale of 0 (no clasping, limbs splayed) to 2 (clasping, wringing paws).

Grip force, an indicator of muscular strength, was measured using a Grip Strength Meter (Columbus Instruments) (Solomon et al., 2013). The meter was positioned horizontally and the mice were held by the base of the tail and lowered towards the triangular pull bar. Once the mice had gripped the bar, the meter was calibrated and the mice were gently pulled away from the apparatus. The force applied to the bar as the mice released it was recorded as peak tension (N). This test was repeated five times with the highest and lowest value being removed for user error and the remaining three values were averaged for the final grip strength.

For the Rotarod task, mice were placed on the Rotarod apparatus (San Diego Instruments) and rotation was increased from 5 rpm to 35 rpm over 5 minutes. Latency to fall was recorded automatically. Ten trials were performed on the first day and four were performed on the second day. There was an inter-trial period of 10 min and during which the mice were placed in their home cage.

Training for the treadmill test occurred over four days (3 min/day). On the first day, the incline was set to 5° and increased by 5° every day to a maximum of 20°. The initial speed was 8 m/min and the treadmill was accelerated by 1 m min^{-2}. On the subsequent training days 2, 3, and 4 the initial speed was increased to 10, 11, and 12 m/min respectively with constant acceleration. During testing on the fifth day, the initial speed was 12 m min^{-1} and accelerated to 20 m min^{-1} over the course of 15 min. Distance to exhaustion was measured and the work performed in Joules (J) was calculated using the formula: W(J) = body weight (kg) x cos20° x 9.8 (J kg^{-1} x m) x distance (m).

In the open field test, locomotor activity was automatically recorded (AccuScan Instrument). The mice were placed in an arena with an area of 20 cm x 20 cm with 30 cm high walls. Mice were acclimated to the locomotor room for ten minutes prior to testing. Locomotor activity was measured in 5 min intervals over 2 h, as previously described (Martyn et al., 2012).

Elevated plus maze, Y-maze, fear conditioning, and novel object recognition.

Animals were placed in the centre of the elevated plus maze (Med Associate Inc) and their activity was recorded over 5 min. Total time spent in the open and closed arms was recorded using computer software (AnyMaze). The centre of the mouse body was used as an indicator of which zone they were in.

Spontaneous Y-maze alternation was measured using a symmetrical three-armed Y-maze as described (de Castro et al., 2009). Video tracking was performed using computer software (AnyMaze) and the order and number of entries into each arm was recorded. Each mouse underwent one trial consisting of five minutes. Spontaneous alternation was counted when a mouse entered all three arms in a row without visiting a previous arm.

To measure contextual fear, mice were placed in a 20 cm x 10 cm clear acrylic enclosure with a metal grid floor and one wall distinct from the others (stripes were drawn on one of the walls). The chamber was equipped with an electric shock generator. Videos were recorded using the AnyMaze video tracking software. On Day 1, mice were allowed to explore the enclosure freely and at 150 s the mice were given a shock (2 mA, 180 V, 2 s). Shock sensitivity was confirmed by vocalization of the mice. 30 s later the mice were returned to their home cage. After 24 h the mice were

placed back into the enclosure for 6 min and freezing time was measured in 30 s intervals. Freezing was defined as immobility lasting more than 0.5 s.

To test novel object recognition, mice were habituated with no objects in an open arena (40 cm x 40 cm) for 5 min on both Day 1 and Day 2. On Day 3, mice were placed in the arena with two identical objects (A, a red plastic ball attached on top of a yellow cube base) and were allowed to explore for 10 min. Video tracking was used (AnyMaze). To test short-term memory, 1.5 h after training mice were placed back in the arena for 5 min with one previous object (A) and one novel object (B, a blue plastic pyramid attached on top of a green prism base). To test long-term memory, 24 h after training mice were placed back in the arena for 5 min with one previous object (A) and one novel object (B). Recognition of previous and novel objects was expressed as percentage of time spent with each object compared to total time interacting. Interaction with the object was defined as sniffing or touching the object, but not leaning against or standing on the object.

Morris Water Maze. The Morris water maze (MWM) was conducted as described previously (Vorhees and Williams, 2006). Mice were given four trials (90 s) a day for 4 consecutive days with a 15 min inter-trial period. The latency to find the platform was recorded using video tracking software (AnyMaze). If the mice did not find the platform during the 90 s, they were gently guided onto the platform. On the fifth and the twelfth day, the platform was removed and time spent in each quadrant of the maze was recorded using the video software. The task was performed in a 1.5 m diameter pool with 25°C water and the platform was submerged 1 cm beneath the water surface. Spatial cues (shapes printed in black & white) were distributed around the pool. For the cued version of the Morris water maze, mice were subjected to 4 trials (90 s) per day for 7 consecutive days with a 30 s inter-trial period. If the mouse did not find the platform after 90 s, it was gently guided onto the platform. The visible platform and the mouse starting location changed with each trial so they were unique between trials. The platform was made visible by placing a red plastic cube on top of the platform which was wiped with ethanol between each trial.

Statistical analyses. All data were analyzed using GraphPad Prism software or SPSS with Student's T test (unpaired, two-tailed) or one or two-way ANOVA with Bonferroni or Benjamini-Hochburg correction where indicated. All results are depicted as mean

+/- SEM unless indicated otherwise. P values of 0.05 or less were considered to indicate significance.

Acknowledgements

We wish to thank Matthew Cowan at the Robarts Neurobehavioural facility for technical assistance. We thank Dr. Michael Miller for his help with statistical analyses. We are also grateful to Doug Higgs and Richard Gibbons for the gift of the *Atrx*$^{f/f}$ mice.

Competing interests

No competing interests declared.

Author contributions

R.J.T. – design, interpretation of data, execution of experiments, writing of article. J.R.S. – execution of experiments, interpretation of data. Y.J. – execution of experiments. M.A.M.P. – interpretation of data, editing of article. F.B. – design, interpretation of data, editing of article. N.G.B. – conception, design, interpretation of data, writing of article.

Funding

This work was supported by a studentship from the Department of Paediatrics at the University of Western Ontario to R.J.T., a Canadian Institutes for Health Research Masters Scholarship to J.R.L. and a Canadian Institutes for Health Research operating grant to N.G.B. (MOP#142369).

Figures

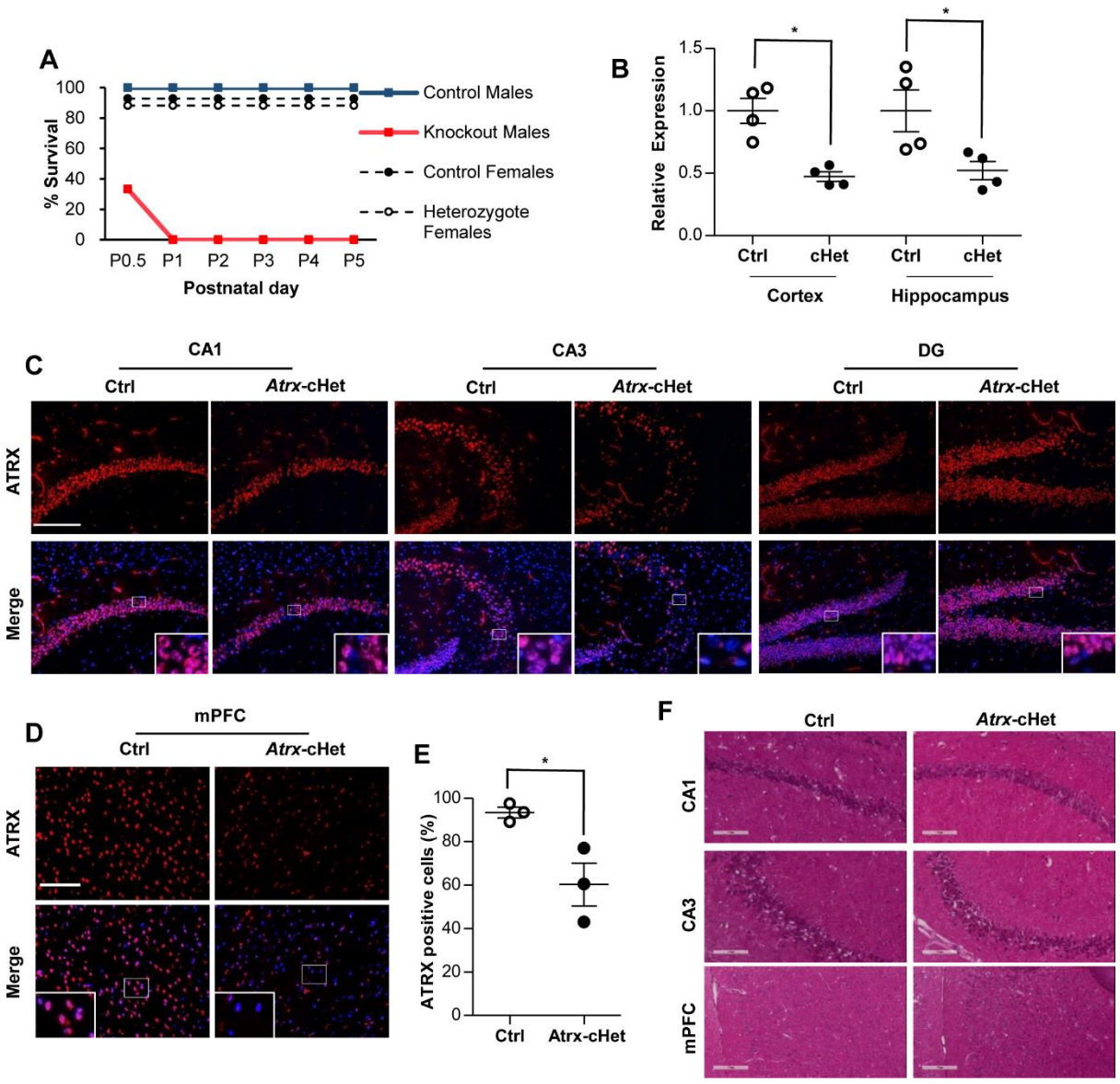

Figure 1: Mosaic pattern of ATRX expression in the brain of Atrx-cHet mice. (A) Graph depicting the survival of control male mice (n=20), knockout male mice (n=6), control female mice (n=14) and heterozygote female mice (n=17) as percent survival at each time point. (B) Reverse transcriptase-qPCR of *Atrx* (normalized to *Gapdh* expression) in the hippocampus and cortex of Atrx-cHet mice and littermate-matched controls (mean +/- S.E.M. of n=4 pairs, two-tailed unpaired T-test). Asterisks indicate

p<0.05. (C) Immunofluorescence staining of ATRX (red) and DAPI (blue) in the hippocampus of control and Atrx-cHet mice. Scale bar, 100μM. CA1: Cornus Ammoni 1, CA3: Cornus Ammoni 3, DG: dentate gyrus. (D) Immunofluorescence staining of ATRX (red) and DAPI (blue) in the medial prefrontal cortex (mPFC) of control and Atrx-cHet mice. Scale bar, 200μM. (E) The percentage of ATRX positive cells in the mPFC of control and Atrx-cHet mice (mean of 3 pairs +/- S.E.M., two tailed unpaired T-test). Asterisk indicates p<0.05. (F) Hematoxylin and eosin staining in the CA1, CA3, and mPFC of control and Atrx-cHet mice. Scale bar, 200 μM.

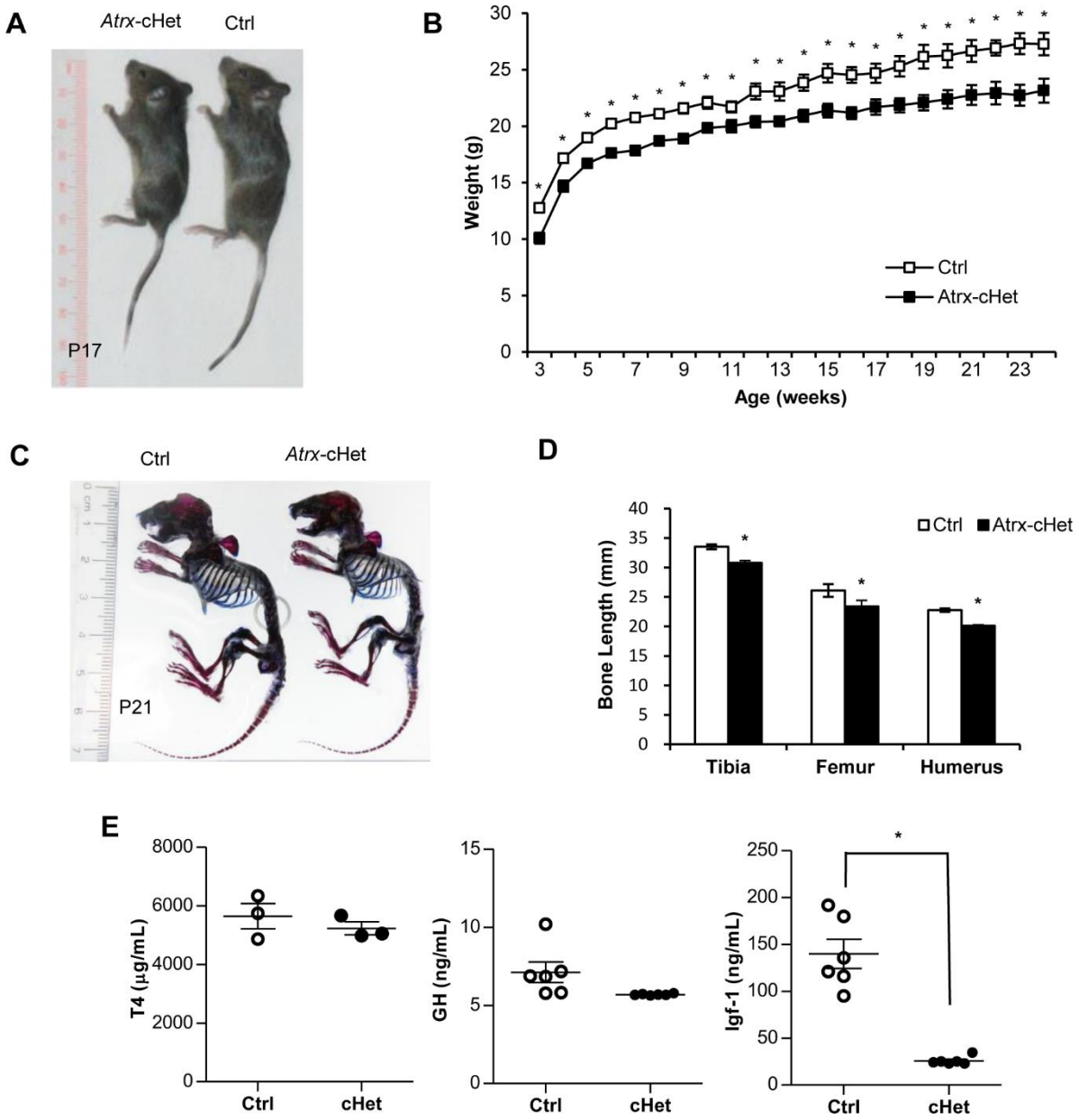

Figure 2. *Atrx*-cHet mice have reduced body weight and low circulating IGF-1. (A) *Atrx*-cHet female mice are smaller than littermate-matched controls at P17. (B) Growth curve of mice from 3 to 24 weeks of age (n=13) ($p<0.05$). Data represented as mean +/- S.E.M, two-way repeated measures ANOVA with Benjamini-Hochburg post-hoc test. (C) Skeletal stains of P21 control and *Atrx*-cHet mice showing cartilage (blue) and bone (red). (D) Long bone length of *Atrx*-cHet mice (n=21) are decreased

compared to control mice (n=19). (E) Circulating levels of T4, GH and IGF-1 in *Atrx*-cHet and control mice (n=3) at P17. Data represented as mean +/- S.E.M., two-tailed, unpaired T-test. Asterisks indicate $p<0.05$.

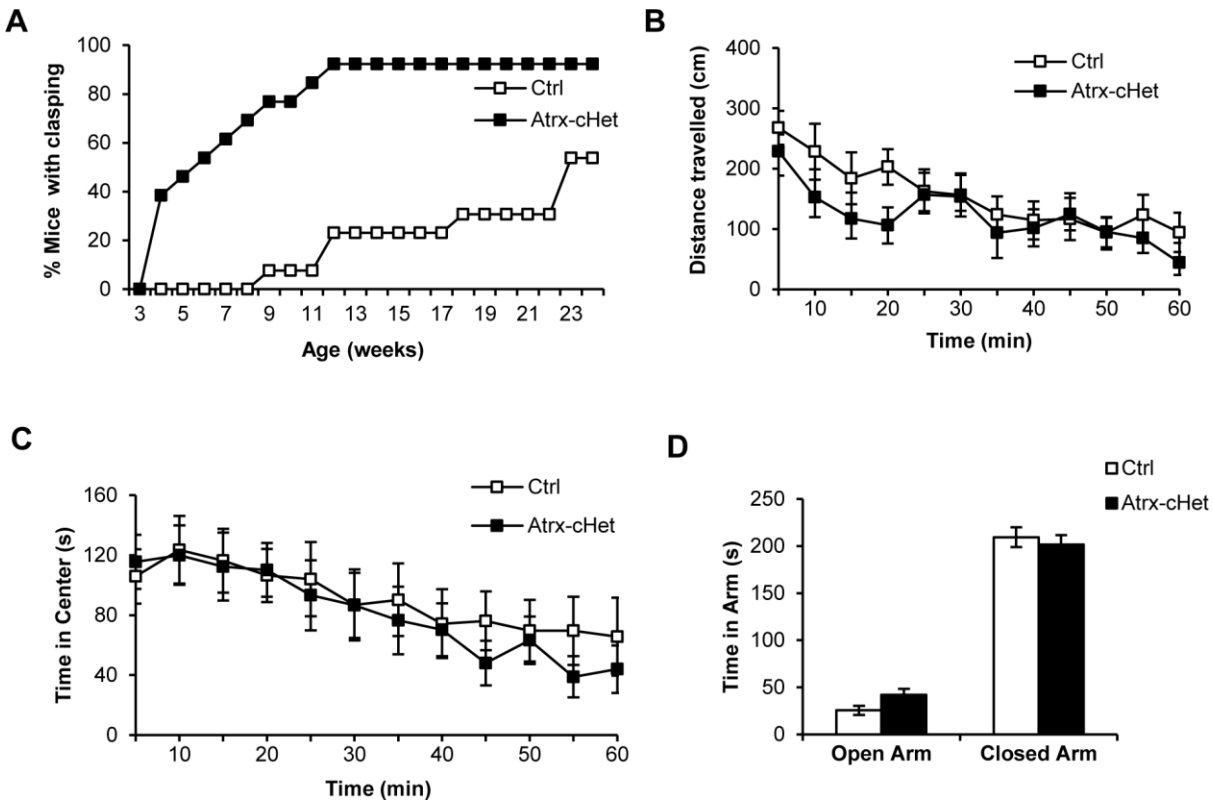

Figure 3. *Atrx*-cHet mice exhibit hindlimb clasping but normal activity and anxiety levels. (A) Hindlimb clasping was evaluated in control (n=13) and *Atrx*-cHet (n=12) female mice and data graphed as the proportion of mice with hindlimb clasping from 3 to 25 weeks of age. Open field test showed no difference in distance travelled (B) and time spent in the centre (C) between control (n=11) and *Atrx*-cHet female mice (n=14). (D) Elevated plus maze paradigm shows no difference in time spent in the open and closed arms in control (n=11) and *Atrx*-cHet (n=13) female mice. The data is represented as mean +/- S.E.M. and a two-way ANOVA test was performed.

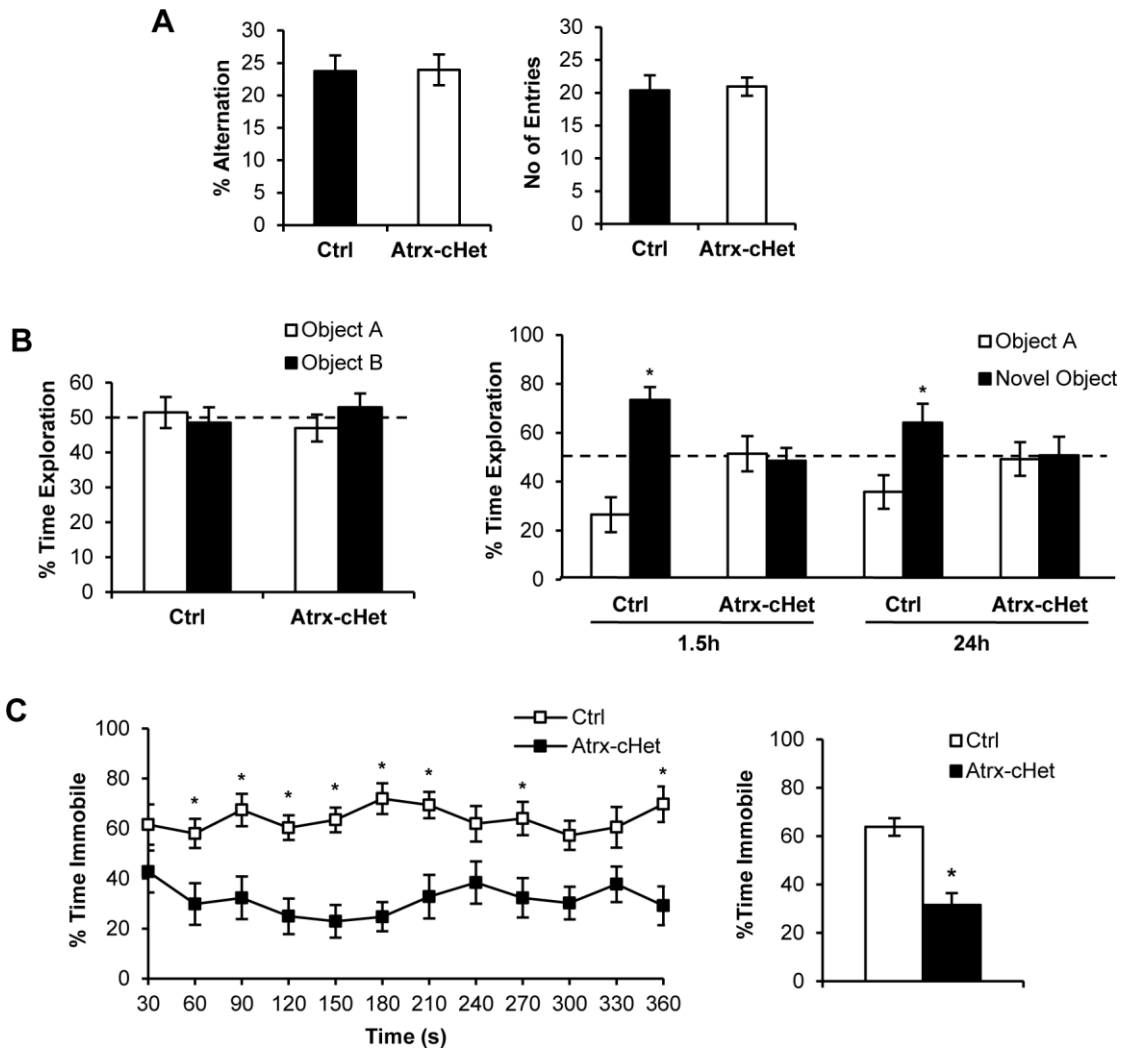

Figure 4. Impaired novel object recognition and contextual fear memory in *Atrx*-cHet mice. (A) Percent alternation and number of arm entries in the Y maze test by control (n=14) and *Atrx*-cHet (n=15) female mice. (B) Control (n=14) and *Atrx*-cHet (n=14) mice displayed similar preference for identical objects in the training session of the Novel Object Recognition task. The Atrx-cHet mice failed to display a preference for the novel object at 1.5h and 24h later ($p<0.05$). (C) *Atrx*-cHet (n=14) mice spent less time immobile than control mice (n=14) in the fear conditioning paradigm. Total percent time spent immobile is shown on the right ($p<0.0001$). Statistical analyses made use of two-tailed, unpaired T-test or two-way ANOVA; data represented as mean +/- S.E.M. and asterisks indicate $p<0.05$.

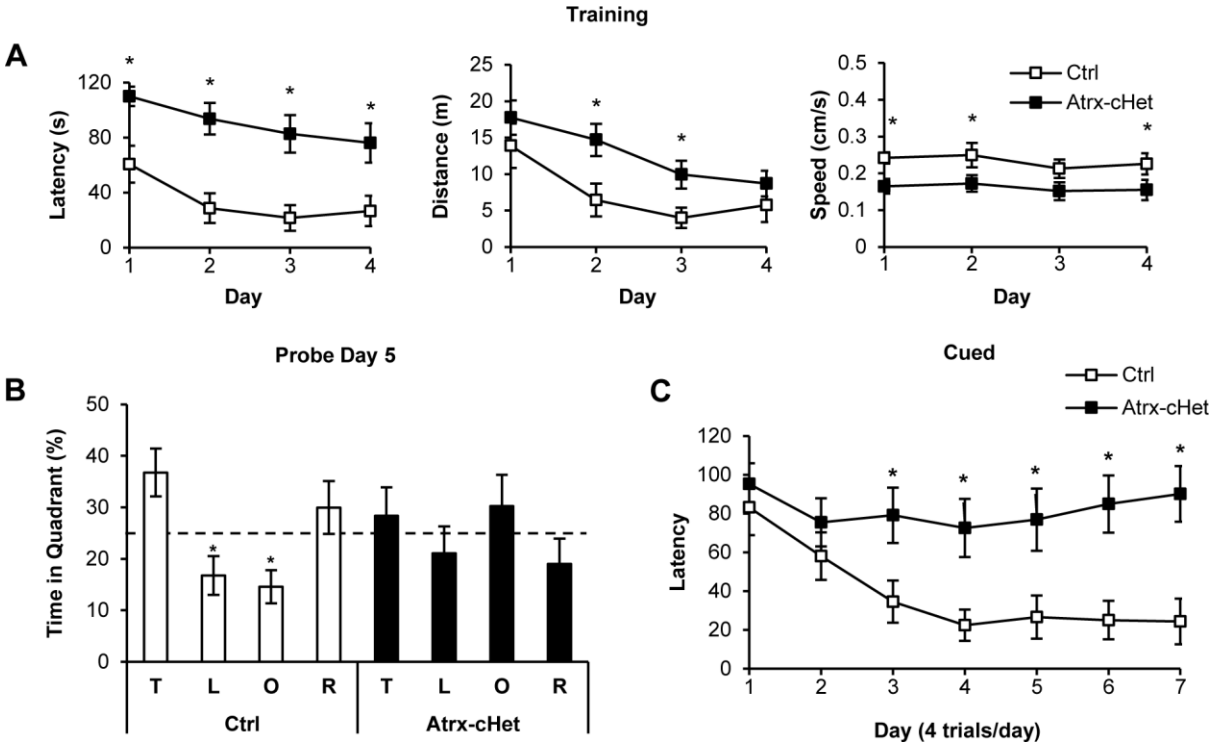

Figure 5. Atrx-cHet mice perform poorly in the Morris water maze paradigm. (A) Atrx-cHet mice (n=13) spent more time finding the platform compared to control mice (n=11) over the four consecutive days of training ($p<0.05$). They swam longer distances but at a lower speed compared to control mice ($p<0.05$). (B) Control mice spent more time swimming in the target quadrant (T) compared to the left (L) and opposite (O) quadrants ($p<0.05$) on the day 5 probe test whereas *Atrx*-cHet mice spent approximately 25% of their time in each of the quadrants. (C) In the cued version of the Morris water maze, Atrx-cHet mice (n=11) were unable to learn the location of the visible platform while the control mice could effectively learn this task (n=11). Data is represented as mean +/- S.E.M. and a two-way ANOVA test was done. Asterisks indicate $p<0.05$.

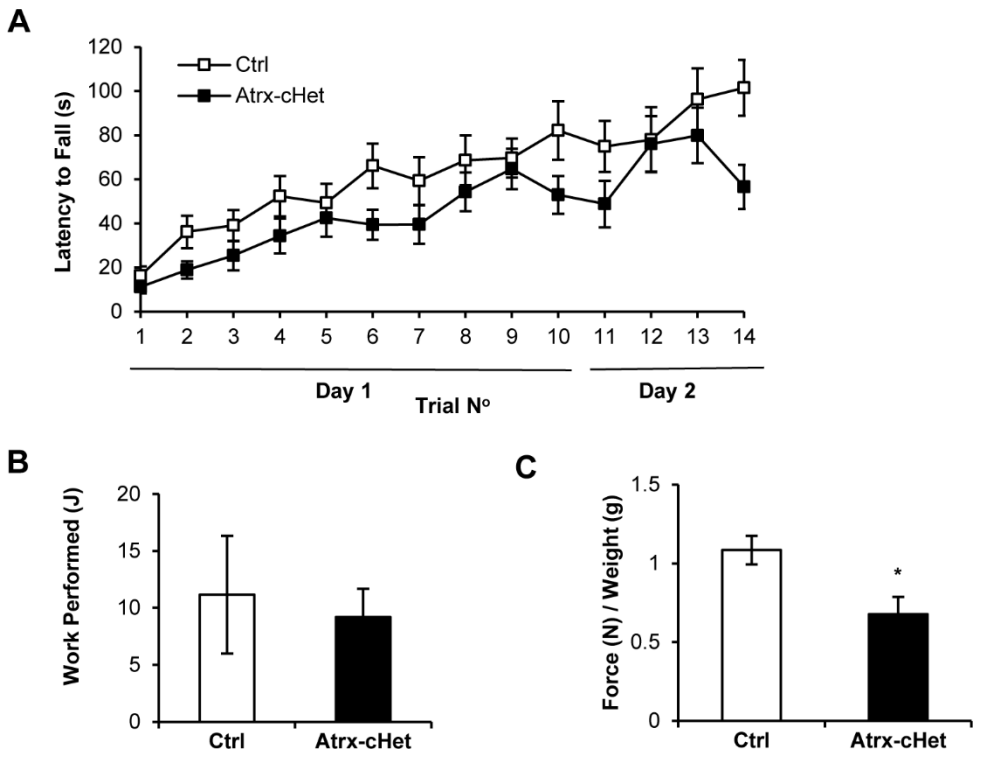

Figure 6. Normal motor memory and endurance but decreased grip strength in Atrx-cHet mice. (A) Atrx-cHet (n=18) and control (n=16) female mice performed normally in the rotarod test. (B) Atrx-cHet (n=15) and control (n=15) mice performed similarly in the treadmill test. (C) Atrx-cHet mice (n=13) exhibit decreased grip strength compared to control mice (n=11), normalized to body weight. Statistical analyses made use of two-way ANOVA or two-tailed, unpaired T-test; data represented as mean +/- S.E.M. and asterisk indicates $p<0.05$.

References:

Aapola, U., Kawasaki, K., Scott, H. S., Ollila, J., Vihinen, M., Heino, M., Shintani, A., Kawasaki, K., Minoshima, S., Krohn, K. et al. (2000). Isolation and initial characterization of a novel zinc finger gene, DNMT3L, on 21q22.3, related to the cytosine-5-methyltransferase 3 gene family. *Genomics* **65**, 293-8.

Berube, N. G., Mangelsdorf, M., Jagla, M., Vanderluit, J., Garrick, D., Gibbons, R. J., Higgs, D. R., Slack, R. S. and Picketts, D. J. (2005). The chromatin-remodeling protein ATRX is critical for neuronal survival during corticogenesis. *J Clin Invest* **115**, 258-67.

Berube, N. G., Smeenk, C. A. and Picketts, D. J. (2000). Cell cycle-dependent phosphorylation of the ATRX protein correlates with changes in nuclear matrix and chromatin association. *Hum Mol Genet* **9**, 539-47.

Bevins, R. A. and Besheer, J. (2006). Object recognition in rats and mice: a one-trial non-matching-to-sample learning task to study 'recognition memory'. *Nat Protoc* **1**, 1306-11.

Cardoso, C., Timsit, S., Villard, L., Khrestchatisky, M., Fontes, M. and Colleaux, L. (1998). Specific interaction between the XNP/ATR-X gene product and the SET domain of the human EZH2 protein. *Hum Mol Genet* **7**, 679-84.

de Castro, B. M., Pereira, G. S., Magalhaes, V., Rossato, J. I., De Jaeger, X., Martins-Silva, C., Leles, B., Lima, P., Gomez, M. V., Gainetdinov, R. R. et al. (2009). Reduced expression of the vesicular acetylcholine transporter causes learning deficits in mice. *Genes Brain Behav* **8**, 23-35.

Declercq, J., Brouwers, B., Pruniau, V. P., Stijnen, P., de Faudeur, G., Tuand, K., Meulemans, S., Serneels, L., Schraenen, A., Schuit, F. et al. (2015). Metabolic and Behavioural Phenotypes in Nestin-Cre Mice Are Caused by Hypothalamic Expression of Human Growth Hormone. *PLoS One* **10**, e0135502.

Dhayalan, A., Tamas, R., Bock, I., Tattermusch, A., Dimitrova, E., Kudithipudi, S., Ragozin, S. and Jeltsch, A. (2011). The ATRX-ADD domain binds to H3 tail peptides and reads the combined methylation state of K4 and K9. *Hum Mol Genet* **20**, 2195-203.

Drane, P., Ouararhni, K., Depaux, A., Shuaib, M. and Hamiche, A. (2010). The death-associated protein DAXX is a novel histone chaperone involved in the replication-independent deposition of H3.3. *Genes Dev* **24**, 1253-65.

Ennaceur, A. and Delacour, J. (1988). A new one-trial test for neurobiological studies of memory in rats. 1: Behavioral data. *Behav Brain Res* **31**, 47-59.

Garrick, D., Sharpe, J. A., Arkell, R., Dobbie, L., Smith, A. J., Wood, W. G., Higgs, D. R. and Gibbons, R. J. (2006). Loss of Atrx affects trophoblast development and the pattern of X-inactivation in extraembryonic tissues. *PLoS Genet* **2**, e58.

Gibbons, R. J., Bachoo, S., Picketts, D. J., Aftimos, S., Asenbauer, B., Bergoffen, J., Berry, S. A., Dahl, N., Fryer, A., Keppler, K. et al. (1997). Mutations in transcriptional regulator ATRX establish the functional significance of a PHD-like domain. *Nat Genet* **17**, 146-8.

Gibbons, R. J., Picketts, D. J., Villard, L. and Higgs, D. R. (1995). Mutations in a putative global transcriptional regulator cause X-linked mental retardation with alpha-thalassemia (ATR-X syndrome). *Cell* **80**, 837-45.

Giusti, S. A., Vercelli, C. A., Vogl, A. M., Kolarz, A. W., Pino, N. S., Deussing, J. M. and Refojo, D. (2014). Behavioral phenotyping of Nestin-Cre mice: implications for genetic mouse models of psychiatric disorders. *J Psychiatr Res* **55**, 87-95.

Grozeva, D., Carss, K., Spasic-Boskovic, O., Tejada, M. I., Gecz, J., Shaw, M., Corbett, M., Haan, E., Thompson, E., Friend, K. et al. (2015). Targeted Next Generation Sequencing Analysis of 1000 Individuals with Intellectual Disability. *Hum Mutat*.

Guy, J., Hendrich, B., Holmes, M., Martin, J. E. and Bird, A. (2001). A mouse Mecp2-null mutation causes neurological symptoms that mimic Rett syndrome. *Nat Genet* **27**, 322-6.

Law, M. J., Lower, K. M., Voon, H. P., Hughes, J. R., Garrick, D., Viprakasit, V., Mitson, M., De Gobbi, M., Marra, M., Morris, A. et al. (2010). ATR-X syndrome protein targets tandem repeats and influences allele-specific expression in a size-dependent manner. *Cell* **143**, 367-78.

Leung, J. W., Ghosal, G., Wang, W., Shen, X., Wang, J., Li, L. and Chen, J. (2013). Alpha thalassemia/mental retardation syndrome X-linked gene product ATRX is required for proper replication restart and cellular resistance to replication stress. *J Biol Chem* **288**, 6342-50.

Levy, M. A., Kernohan, K. D., Jiang, Y. and Berube, N. G. (2015). ATRX promotes gene expression by facilitating transcriptional elongation through guanine-rich coding regions. *Hum Mol Genet* **24**, 1824-35.

Lewis, P. W., Elsaesser, S. J., Noh, K. M., Stadler, S. C. and Allis, C. D. (2010). Daxx is an H3.3-specific histone chaperone and cooperates with ATRX in replication-independent chromatin assembly at telomeres. *Proc Natl Acad Sci U S A* **107**, 14075-80.

Logue, S. F., Paylor, R. and Wehner, J. M. (1997). Hippocampal lesions cause learning deficits in inbred mice in the Morris water maze and conditioned-fear task. *Behav Neurosci* **111**, 104-13.

Margueron, R., Justin, N., Ohno, K., Sharpe, M. L., Son, J., Drury, W. J., 3rd, Voigt, P., Martin, S. R., Taylor, W. R., De Marco, V. et al. (2009). Role of the polycomb protein EED in the propagation of repressive histone marks. *Nature* **461**, 762-7.

Martyn, A. C., De Jaeger, X., Magalhaes, A. C., Kesarwani, R., Goncalves, D. F., Raulic, S., Guzman, M. S., Jackson, M. F., Izquierdo, I., Macdonald, J. F. et al. (2012). Elimination of the vesicular acetylcholine transporter in the forebrain causes hyperactivity and deficits in spatial memory and long-term potentiation. *Proc Natl Acad Sci U S A* **109**, 17651-6.

Michod, D., Bartesaghi, S., Khelifi, A., Bellodi, C., Berliocchi, L., Nicotera, P. and Salomoni, P. (2012). Calcium-dependent dephosphorylation of the histone chaperone DAXX regulates H3.3 loading and transcription upon neuronal activation. *Neuron* **74**, 122-35.

Morris, R. (1984). Developments of a water-maze procedure for studying spatial learning in the rat. *J Neurosci Methods* **11**, 47-60.

Nan, X., Hou, J., Maclean, A., Nasir, J., Lafuente, M. J., Shu, X., Kriaucionis, S. and Bird, A. (2007). Interaction between chromatin proteins MECP2 and ATRX is disrupted by mutations that cause inherited mental retardation. *Proc Natl Acad Sci U S A* **104**, 2709-14.

Nogami, T., Beppu, H., Tokoro, T., Moriguchi, S., Shioda, N., Fukunaga, K., Ohtsuka, T., Ishii, Y., Sasahara, M., Shimada, Y. et al. (2011). Reduced expression of the ATRX gene, a chromatin-remodeling factor, causes hippocampal dysfunction in mice. *Hippocampus* **21**, 678-87.

Phillips, R. G. and LeDoux, J. E. (1992). Differential contribution of amygdala and hippocampus to cued and contextual fear conditioning. *Behav Neurosci* **106**, 274-85.

Picketts, D. J., Higgs, D. R., Bachoo, S., Blake, D. J., Quarrell, O. W. and Gibbons, R. J. (1996). ATRX encodes a novel member of the SNF2 family of proteins: mutations point to a common mechanism underlying the ATR-X syndrome. *Hum Mol Genet* **5**, 1899-907.

Ritchie, K., Watson, L. A., Davidson, B., Jiang, Y. and Berube, N. G. (2014). ATRX is required for maintenance of the neuroprogenitor cell pool in the embryonic mouse brain. *Biol Open* **3**, 1158-63.

Seah, C., Levy, M. A., Jiang, Y., Mokhtarzada, S., Higgs, D. R., Gibbons, R. J. and Berube, N. G. (2008). Neuronal death resulting from targeted disruption of the Snf2 protein ATRX is mediated by p53. *J Neurosci* **28**, 12570-80.

Solomon, L. A., Russell, B. A., Watson, L. A., Beier, F. and Berube, N. G. (2013). Targeted loss of the ATR-X syndrome protein in the limb mesenchyme of mice causes brachydactyly. *Hum Mol Genet* **22**, 5015-25.

Stearns, N. A., Schaevitz, L. R., Bowling, H., Nag, N., Berger, U. V. and Berger-Sweeney, J. (2007). Behavioral and anatomical abnormalities in Mecp2 mutant mice: a model for Rett syndrome. *Neuroscience* **146**, 907-21.

Tronche, F., Kellendonk, C., Kretz, O., Gass, P., Anlag, K., Orban, P. C., Bock, R., Klein, R. and Schutz, G. (1999). Disruption of the glucocorticoid receptor gene in the nervous system results in reduced anxiety. *Nat Genet* **23**, 99-103.

Ulici, V., Hoenselaar, K. D., Agoston, H., McErlain, D. D., Umoh, J., Chakrabarti, S., Holdsworth, D. W. and Beier, F. (2009). The role of Akt1 in terminal stages of endochondral bone formation: angiogenesis and ossification. *Bone* **45**, 1133-45.

Vorhees, C. V. and Williams, M. T. (2006). Morris water maze: procedures for assessing spatial and related forms of learning and memory. *Nat Protoc* **1**, 848-58.

Wan, H., Aggleton, J. P. and Brown, M. W. (1999). Different contributions of the hippocampus and perirhinal cortex to recognition memory. *J Neurosci* **19**, 1142-8.

Watson, L. A., Solomon, L. A., Li, J. R., Jiang, Y., Edwards, M., Shin-ya, K., Beier, F. and Berube, N. G. (2013). Atrx deficiency induces telomere dysfunction, endocrine defects, and reduced life span. *J Clin Invest* **123**, 2049-63.

Wiese, C., Rolletschek, A., Kania, G., Blyszczuk, P., Tarasov, K. V., Tarasova, Y., Wersto, R. P., Boheler, K. R. and Wobus, A. M. (2004). Nestin expression--a property of multi-lineage progenitor cells? *Cell Mol Life Sci* **61**, 2510-22.

Xing, W., Govoni, K. E., Donahue, L. R., Kesavan, C., Wergedal, J., Long, C., Bassett, J. H., Gogakos, A., Wojcicka, A., Williams, G. R. et al. (2012). Genetic evidence that thyroid hormone is indispensable for prepubertal insulin-like growth factor-I expression and bone acquisition in mice. *J Bone Miner Res* **27**, 1067-79.

Xue, Y., Gibbons, R., Yan, Z., Yang, D., McDowell, T. L., Sechi, S., Qin, J., Zhou, S., Higgs, D. and Wang, W. (2003). The ATRX syndrome protein forms a chromatin-remodeling complex with Daxx and localizes in promyelocytic leukemia nuclear bodies. *Proc Natl Acad Sci U S A* **100**, 10635-40.

Zhang, J., Ji, F., Liu, Y., Lei, X., Li, H., Ji, G., Yuan, Z. and Jiao, J. (2014). Ezh2 regulates adult hippocampal neurogenesis and memory. *J Neurosci* **34**, 5184-99.